AD-A190 508 ANTHROPOMORPHIC PHANTOM RADIATION DOSIMETRY AT THE NATO 1/1
STANDARD REFERENC (U) DEFENCE RESEARCH ESTABLISHMENT
OTTAWA (ONTARIO) T COUSINS EE AL APR 87 DREO-968

UNCLASSIFIED F/G 6/7 NL

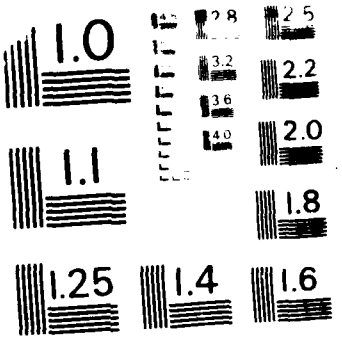
1.0
1.1
1.25
1.4
1.6
1.8
2.0
2.2
2.5
2.8
3.2
3.6
4.0

National Defence / Défense nationale

ANTHROPOMORPHIC PHANTOM RADIATION DOSIMETRY AT THE NATO STANDARD REFERENCE POINT AT ABERDEEN PROVING GROUND

by

T. Cousins and L.P. Rushton

DEFENCE RESEARCH ESTABLISHMENT OTTAWA
REPORT NO. 968

April 1987
Ottawa

Canada

National Defence / Defense nationale

ANTHROPOMORPHIC PHANTOM RADIATION DOSIMETRY AT THE NATO STANDARD REFERENCE POINT AT ABERDEEN PROVING GROUND

by

T. Cousins and L.P. Rushton
Nuclear Effects Section
Protective Sciences Division

DEFENCE RESEARCH ESTABLISHMENT OTTAWA
REPORT NO. 968

PCN
051LA

April 1987
Ottawa

ABSTRACT

As part of the NATO Dosimetry Intercomparison Project, a series of experiments were conducted at Aberdeen Proving Ground in September 1986 in order to determine neutron and gamma-ray doses delivered to various internal and external locations on an anthropomorphic phantom from a fission source. Thus the effect of such parameters as self-shielding by the body on dosimeter reading may be determined. The results will be used eventually to validate computer simulations of the Aberdeen environment in order to understand completely the correlation between dosimeter reading and bone marrow dose, or other parameters relating to performance decrement.

RESUME

En septembre 1986, à Aberdeen Proving Ground, nous avons effectué une série de tests dans le but de déterminer les doses neutron et les doses gamma à différents endroits internes et externes d'un mannequin anthropomorphe en utilisant un réacteur nucléaire. A la suite de ces tests, nous pourrons déterminer l'effet de l'autoblindage du mannequin sur la lecture des dosimètres. Nous utiliserons ensuite ces résultats pour les comparer avec les résultat des simulations théoriques afin de comprendre les corrélations qui existent entre la lecture d'un dosimètre et la dose de la moëlle osseuse et les paramètres qui pourraient amoindria le rendement d'un soldat.

Introduction

The need to establish the relationship between the measured dose from a military dosimeter, worn at a particular location on a soldier's body, and the corresponding expected biological effects (leading to performance decrement) should be readily apparent. Whether this dosimeter reading should be related to free-field dose as suggested in current STANAGs (1) or to some particular organ of biological significance (such as bone marrow (2)) is a question generating much lively debate. In either case, the solution to the problem requires both theoretical and experimental work.

The major thrust of the theoretical calculations thus far has been performed by Kaul et al ((3),(4),(5)) wherein the dose distribution both within and on a computer-simulated standard man was determined at large (~1 km) distances from simulated standard fission weapon bursts of 5-100 kT occurring at a height of 278 m. The results here have demonstrated that, depending on the man's orientation with respect to the explosion, variations in dosimeter response of up to roughly 40% may be expected. Experimental verification of these results directly is, fortunately, impossible. In addition, at present, there is no research facility capable of raising a reactor to such a great height and still give measurable doses at such large distances.

Thus, as a compromise, it was decided to perform dosimetric measurements on an anthropomorphic phantom located at the NATO standard reference point 400 m from the fission core at the Nuclear Effects Directorate (NED), Aberdeen Proving Ground, Md. (6), about which more will be said later. The computer calculations could then be re-tailored to the Aberdeen scenario, and a direct comparison could ensue.

Previous experiments have been carried out at NED to determine such doses at both close-in (7) and NATO standard distances (8,9). Recent advances, however, allow much more accurate (and precise) determination of both neutron and gamma-ray doses of the levels which occur at the 400-m position. DREO decided to employ two types of neutron dosimeters and one type of gamma-ray dosimeter on its anthropomorphic phantom for the work. A concurrent experiment undertaken by French (ETCA) scientists utilized slightly different dosimeters and phantom. The results presented here represent DREO's experimental data. A comparison with results of computer calculations by Science Applications Incorporated (SAI) will follow when these are available. The results of the ETCA experiment will be presented elsewhere.

EXPERIMENTAL EQUIPMENT

(1) Anthropomorphic Phantom

The phantom previously employed by DREO (Alderson 'REMAB' model (7)) had in recent years become increasingly difficult to use because of increased occurrence of leaks at seams due to temperature-related stresses during long runs. As a result DREO purchased a new solid anthropomorphic phantom - the

Humanoid RT-200 (Humanoid Systems, Carson, California) which has proved much more utilitarian as a research tool. A summary of the salient features of the phantom are given below.

The construction of the RT-200 phantom embraces an anatomically correct 50th percentile male human skeleton encased in a plastic "body". The body is sliced into 2.5 cm (0.98") sections which are held together by nylon rods when the phantom is assembled. Each slice is "gridded" into a 1" matrix of removable plugs which facilitate easy insertion of small dosimeters (such as TLDs) at virtually any internal location. The slicing of the plastic applied to the torso, head, arms and legs of the phantom. The hands and feet were of one-piece construction.

The efficacy of a phantom for radiation dosimetry is governed by the elemental composition of its plastic corresponding as closely as possible to that of standard man. The manufacturer claimed that the HCNO - Hydrogen, Carbon, Nitrogen and Oxygen composition of their plastic was matched as closely as possible to the quoted values in ICRP 23 (10) (with no other contaminants to greater than 1% by mass) but offered no numerical data to back up this claim. Accordingly, DREO had a chemical analysis conducted by Guelph Chemical Laboratories, Guelph, Ontario to determine H,C and N concentrations. In addition neutron activation analysis (NAA) tests were carried out at the SLOWPOKE reactor at Royal Military College, Kingston, to ascertain the levels of any contaminants. The plastics of the RT-200 were a "body" plastic filling most of the frame, and a "lung" plastic representing the somewhat less dense lung component. The results of these analyses are given in tables (1) and (2).

The elemental composition of the body plastic does compare favourably with SHONKA A-150 plastic as a close match to standard man, especially in terms of the important (for neutron dosimetry) H content. The lung plastic is not quite as close a match but this is not viewed as critical because of the smaller volume occupied by the lungs and the large variations in the ICRP quoted compositions. Trace compositions are indeed very low and this augurs well for experimental work. It should be noted that the theoretical standard man and RT-200 compositions could be readily interchanged and any differences in dosimeter response due to these elemental differences could thus be observed.

(2) DOSIMETERS

The dosimeter/reader systems used here are all to some degree improved versions of previously employed systems. The most marked improvement over the recent years has been in neutron dosimetry, with the detectors described below allowing much greater sensitivity and precision in measurements. A brief outline of the pertinent features of the three types of dosimeters is now given.

TABLE 1

RESULTS OF ELEMENTAL ANALYSIS OF RT-200
PLASTICS AND COMPARISON WITH OTHER MATERIALS

% BY MASS

	H	C	N	O*
RT-200 'BODY'	9.6	65.4	4.5	(20)
SHONKA A-150	10.1	77.6	3.5	5.2
LUCITE	8.0	60.0	-	32.0
[10]TISSUE APPROX	10.0	14.9	3.5	71.6
[10]TISSUE MUSCLE	10.2	12.3	3.5	72.9
[10]TISSUE, ST. MAN	10.0	18.0	3.0	65.0
RT-200 'LUNG'	7.1	60.6	6.1	(26)
[10]ICRP LUNG	9.9	10.0	2.8	74.0

*INFERRED FROM SUBTRACTION FOR RT-200

- NO DIRECT MEASUREMENT FOR OXYGEN

TABLE 2

TRACE ELEMENT COMPOSITIONS OF RT-200 PLASTICS AS DETERMINED BY N.A.A.[11]

'LUNG' PLASTIC

ELEMENT	ppm
Na	17 ± 3
Al	15.6 ± 0.7
Mn	-
Cl	1076 ± 18
Br	11.6 ± 0.8

'BODY' PLASTIC

ELEMENT	ppm
Na	864 ± 24
Al	10.2 ± 0.4
Mn	0.77 ± 0.06
Cl	135 ± 3
Br	-

(2.1) GAMMA RAY DOSIMETRY

CaF_2:Mn Thermoluminescent Dosimeters have been employed in the past for dosimetry at NED (9). The improvement made for this work was the use of a newly acquired Harshaw 2000A (heater)/2080 picoprocessor reading system. The advantages of the new system over the older DREO system (12) lie in its portability, data storage capabilities, low background and its glow curve display/selective integration features. In order to increase still further the accuracy of the system, twenty TLD chips were hand-picked at DREO for their precision when exposed to doses expected to be encountered at NED. The results of these tests are presented in table (3). For these experiments the chips were exposed to known doses at measured distances from DREO's calibrated GRM-750 ^{60}Co source. Electronic equilibrium was assured here by the use of an appropriate thickness of plastic material surrounding the dosimeters.

TABLE 3

DOSE-LINEARITY CHECK OF CaF_2:Mn TLDs
WITH NEW DREO SYSTEM

DOSE*	MEASURED CHARGE/DOSE
10 mR	0.201 $\pm$ .005 nc/mR
20 mR	0.204 $\pm$ .009 nc/mR
33 mR	0.202 $\pm$ .006 nc/mR
50 mR	0.213 $\pm$ .007 nc/mR

average 0.205 $\pm$ .003 nc/mR

*delivered with calibrated ^{60}Co source (GRM-750)

Finally the energy dependence of the chips (while wrapped in tin energy-compensation shields (12)) was determined. Exposure to ^{60}Co, ^{137}Cs and low energy X-ray sources was undertaken. The results of these experiments are shown in Fig (1).

(2.2) NEUTRON DOSIMETRY

The neutron dosimeters used here were of two kinds - the super-heated drop "bubble" detector recently developed at Chalk River Nuclear Laboratories by H. Ing (13) and a CR39 solid-state track-detector system (14). Both had been employed with some success in earlier experiments at NED (8,14), however recent advances in both technologies allowed for much more accurate determinations of neutron doses in the 10-100 mRad range. This increased efficiency is viewed as critical since this represents the range of doses which may be achieved in reasonable time periods at the 400m position.

As always, the dose-energy dependent response of each detector needed to be determined before the actual experiments. Toward this end, both dosimeters were exposed to neutrons spanning the energy range 100 keV-16 MeV produced at the DREO Van de Graaff facility. The results of these tests are presented for the bubble dosimeters and CR39 in figs. (2) and (3) respectively. Note that the CR39 is much flatter in terms of Kerma response than the bubble detector. However, the claim that the bubble detector offers a flat (tissue-equivalent) response in terms of dose-equivalent is borne out upon examination of fig (4). Note especially here that the manufacturer's claimed sensitivity of 1.65 bubbles/mrem is indeed verified to within statistical uncertainties over the entire energy range.

Brief mention should be made of the relative advantages and disadvantages of the two dosimeters. The bubble dosimeter, being a volume detector, is isotropic in its angular response, whereas the CR39 (surface) dosimeter will have a non-isotropic angular dependance. Thus, for free-field dosimetry, while the bubble detector results could be directly transformed into kerma, special care had to be taken for the CR39 values. The method chosen here to circumvent the angular problem is based on an examination of the measured angular response of CR39 shown in fig (5). Note the overlay of a pure cos θ response. The agreement between the two is good up to 45°, and this accord allows simplifying assumptions as below.

For free-field dosimetry at NED, three orthogonal CR39 foils were irradiated simultaneously, and assuming a cos θ response, the three components were added quadratically to give the total dose i.e.

$$D_{total} = \sqrt{(D_x)^2 + (D_y)^2 + (D_z)^2}$$

Calculations were carried out to see how much error this kind of an assumption would make. For a completely isotropic field, this above method would underestimate the actual dose by roughly 15%. However, for a radiation field such as would be encountered at NED, where the majority of neutrons are incident normally on one face, this underestimate can easily be shown to be of the order of 5%. One advantage of the use of foil detectors is, in fact, a direct measurement of neutron anisotropy - an experiment which has never been successfully undertaken. This too may eventually be compared to the theoretical calculations.

The main drawback of the bubble detectors lies in their marked sensitivity variation as a function of temperature as shown in fig (6). During the course of the actual NED experiments, the detectors were always shielded from direct sunlight to prevent direct heating, and the air (or phantom surface) temperature was accurately monitored. However, some variations may have occurred and unforeseen errors may have crept in.

2.3 Dosimeter Location

The choices of dosimeter location were governed by their proximity to both organs of interest and some suggested body sites at which dosimeters should be worn in the field. However a major consideration was not to overburden the phantom, and thus run the risk of the dosimeters themselves being a major self-shielding consideration. In order to increase the statistical accuracy of the results, three bubble dosimeters, two CR39 and two TLDs were used at each external location. In addition, two TLDs were used at the mid-brain and mid-line gut locations. Due to machining and size limitations, no neutron dosimetry was performed at the midbrain location, while at the mid-line gut location only one of each type of neutron dosimeter was feasible. The CR39 mid-line gut dosimeter was oriented parallel to the plane of the hips.

A list of all phantom dosimeter locations, and associated abbreviations which will be referenced later is given in Table (4).

TABLE 4

PHANTOM DOSIMETER LOCATIONS
(See Figures for Clarification)

Chest (CH) - assume left side unless stated explicitly CH(L) or CH(R)

Belt (Front) (BE)

Right Wrist (RW)

Left Wrist (LW)

Lower Back (LB)

Mid-Line Gut (MG)

Mid-Brain (MB) - TLDs only

A total of four phantom orientations were used, namely:

(a) Phantom facing the core (0°)
(b) Phantom rotated 90°, so that right-hand side faces core
(c) Phantom rotated 180°, so that the back was toward the core
(d) Phantom prone (with arms extended over head) (at 0°)

Figs (7) (8) and (9) should clarify the phantom orientations and dosimeter positions.

(3) Experimental Procedures

The three types of dosimeters have somewhat different sensitivities, and thus differing irradiation times (or integrated power levels) were required. These times were determined from the results of previous experiments, in order to give an amenable dose to each detector. At 400 m it was deduced that, at 6 kW, a 20 min irradiation would produce a statistically significant number of bubbles, whereas 2 hrs was required by both the TLDs and CR39. All values of Kerma reported herein are normalized to kWh to facilitate ready comparison.

(4) Results

4.1 Free-Field Kerma Values

The need for accurate free-field dosimetry should be apparent for two reasons. Firstly, a great deal of experimental and theoretical work has already been done in order to determine the free-field neutron and gamma-ray kermas at 400 m. Thus the results presented here may be compared directly with other values in order to demonstrate the efficacy of the method. Secondly, by measuring the free-field kerma for each run, transmission factors may be directly determined precluding the need for any assumptions concerning constancy and reproducibility of power levels.

On the basis of Science Application Incorporated (SAI) calculated neutron and gamma-ray spectra (15), the predicted detector response P (in bubble, track cm^{-2} or charge) for each experimental run could be determined as

$$P = C \int_{}^{20\ MeV} K(E)\Phi(E)\ R(E)dE$$

where $\Phi(E)$ = calculated particle fluence at 400 m for integrated power
$R(E)$ = detector response in (bubbles) (track cm^{-2}) (charge) /mrad
$K(E)$ = Kerma to fluence conversion factor
C = temperature correction factor for bubble dosimeters

(C = 1 for CR39 and TLDs)

Table (5) gives these predicted values compared to the actual experimental values.

The results for the neutron dosimeters are seen to agree extremely well with the predicted values. The gamma-ray results are in general slightly higher than the predicted ones, which may be due to some interference from neutron-generated gamma-rays originating in the phantom itself. The fact that the lowest TLD value occurs when the phantom is prone, and thus further away from the dosimeters tends to support this theory. The overall average of the TLD measured charge would be (3.99 $\pm$ .29) nC, in good agreement with the theory.

TABLE 5

COMPARISON OF MEASURED TO PREDICTED FREE-FIELD DETECTOR RESPONSES

Dosimeter	Predicted Response	Measured Response Phantom Orientation			
		a	b	b	d
Bubble	90 Bubbles	89 ± 5	87 ± 3	84 ± 3	95 ± 3
CR39	252.5 t-cm^{-2}	259 ± 7	294 ± 4	237 ± 3	236 ± 2
TLD	.320 nC	.353 ± .023	.349 ± .013	.327 ± .016	.30 ± .007

RELATIVE DETECTOR RESPONSES FOR 2 HR RUNS
(INTEGRATED POWER = 12 kWh)

Phantom Orientation	Relative Response TLD	CR39
(a)	1.00	1.00
(b)	0.99	0.96
(c)	0.93	0.91
(d)	0.85	0.90

It is interesting to examine reproducibility of power levels, as in table 6. Note that both the neutron and gamma-ray dosimeters track each other quite closely. However, since neither dosimeter should be taken as better than ± 10% in accuracy, it would not be prudent to draw any conclusions concerning this reproducibility. It does suggest, however, than an alternate, independent method of monitoring neutron fluence should be considered. The Rh-foil activation method developed and used by CRNL (16,17) would seem a good candidate here.

Finally the viability of each detector as a direct dosimeter is examined in table (7). In arriving at the values here, the average responses (per mrad) were used for CR39 and TLDs. For the bubble dosimeters, the manufacturer's response (per mrem) was used, and then converted to mrad using a factor of 12.44 for a fission spectrum (18).

TABLE 7

AVERAGE DOSIMETER RESPONSES COMPARED
TO EXPERIMENT AND THEORY

Method	mrad/kWh	
	Neutron	Gamma Ray
Theoretical Calculations	5.0	1.34
DREO Spectroscopy	4.8 ± .3	1.39 ± .04
Bubble Dosimeters	4.50 ± .48	
CR39	4.63 ± .4	
TLD		1.47 ± .11

The experimental results are compared to both the theoretical calculations and the results of DREO's latest spectroscopic measurements. The results are again seen to be in excellent agreement.

4.2 Phantom Dosimetric Results

The phantom dosimeter results are shown in tables (8), (9) and (10) for TLD, bubble and CR39 detectors respectively. These results are discussed for each dosimeter below.

(a) TLD results

Table 8(a) gives the measured charge for each dosimeter for each orientation. The errors here represent the statistical variation on the two individual TLD measurements. Table 8(b) gives the ratios of the TLD values at each phantom position to the free-field response for that particular run. Based upon the slight energy variation in dosimeter response, we estimate the error on these numbers to be of the order of 5%. In addition, for orientations (b) and (c), minor noise difficulties manifested themselves in the reader system. However, even for these two runs, it is not felt that the errors would increase significantly, and would still be well under 10%.

TABLE 8

(a) TLD results for phantom dosimetry - all values shown are measured charge (in nC)

	Phantom Orientation			
TLD Location	(a)	(b)	(c)	(d)
free-field	4.23 ± .28	4.19 ± .15	3.92 ± .18	3.60 ± .08
CH	6.32 ± .27	5.81 ± .37	5.09 ± .14	4.90 ± .06
BE	5.19 ± .02	4.56 ± .23	4.07 ± .48	3.34 ± .02
RW	4.43 ± .27	4.69 ± .07	4.26 ± .18	3.98 ± .05
LW	4.62 ± .07	3.67 ± .11	4.17 ± .16	3.71 ± .08
LB	3.91 ± .02	4.68 ± .01	4.99 ± .35	4.11 ± .02
UB	-	4.80 ± .10		
MG	5.14	4.92	4.99	3.06
MB	5.40	5.28	5.57	5.14

(b) Ratio of Phantom Response (nC) to FF Response (nC)

	Phantom Orientation			
TLD Location	(a)	(b)	(c)	(d)
CH	1.49	1.39	1.30	1.36
BE	1.23	1.09	1.04	0.93
RW	1.05	1.12	1.09	1.11
LW	1.09	0.88	1.06	1.03
LB	0.92	1.12	1.27	1.14
UB		1.15		
MG	1.22	1.17	1.27	0.85
MB	1.28	1.26	1.42	1.43

TABLE 9

(a) Bubble dosimeter responses for phantom dosimetry
(all values shown are in (temperature corrected) $\frac{\text{bubbles}}{\text{kWh}}$)

		Phantom Orientation			
Bubble Dosimeter Location		(a)	(b)	(c)	(d)
free-field		89 ± 5	87 ± 3	84 ± 3	95 ± 3
CH(L)		94 ± 8	65 ± 4	60 ± 2	40 ± 2
CH(R)			73 ± 6	60 ± 3	41 ± 3
BE		91 ± 11	68 ± 2	57 ± 4	28 ± 3
RW/LW	(1)	97/85		100/98	
	(2)		68 ± 3/46 ± 5		95 ± 6/96 ± 5
	(3)	64/61		84/87	
LB		28 ± 5	56 ± 1	92 ± 5	90 ± 2
MG		12	9	16	8

(b) Ratios of Phantom Response (bubbles)
to FF Response (bubbles)

		Phantom Orientation			
Bubble Dosimeter Location		(a)	(b)	(c)	(d)
CH(L)		1.06	.75	.71	.42
CH(R)			.84	.71	.43
BE		1.03	.78	.68	.29
RW/LW	(1)	1.09/.96		1.19/1.17	
	(2)		.78/.53		1.00/1.01
	(3)	.72/.69		1.00/1.04	
LB		.31	.64	1.10	.95
MG		.13	.10	.19	.08

TABLE 10

CR39 Dosimeter Responses in (tracks cm^{-2} kwh^{-1})

	Phantom Orientation			
Dosimeter Location	(a)	(b)	(c)	(d)
FF x	203. ± 5.3	197.7 ± 14.7	185.3 ± 0.3	180.4 ± 0.9
FF y	108.9 ± 3.5	108.4 ± 15.3	99.8 ± 3.1	107.8 ± 4.4
FF z	118.2 ± 2.8	104.9 ± 2.2	109.3 ± 2.9	107.1 ± 6.5
CH	160.8 ± 1.2	71.1 ± 1.8	89.9 ± 7.9	44.4 ± 2.8
BE	148.5 ± 2.5	69.6 ± 1.8	80.2 ± 4.0	36.5 ± 4.0
RW	91.4 ± 5.3	149.3 ± 11.9	87.0 ± 3.5	86.1 ± 5.7
LW	93.6 ± 7.1	67.4 ± 3.5	87.0 ± 1.3	83.5 ± 6.6
LB	100.1 ± 1.9	75.2 ± 2.2	153.3 ± 5.7	88.3 ± 5.7
MG	30.5	21.2	35.8	16.3

x = perpendicular to core - 400 m ray
y = parallel to core - 400 m ray
z = parallel to air-ground interface

Several comments should be made about these results. The expected trends are readily seen, i.e. a dosimeter on the side of the phantom facing the core shows a consistently higher reading than a correspondingly placed TLD on the side of the phantom away form the core. The on (and in) phantom dosimeters in general give results higher than the free-field values, indicating that neutron scattering and capture processes in the plastic are predominant over gamma-ray attenuation with the exceptions here being only when the entire body mass shields the dosimeter.

One interesting feature is that the dosimeter located on the chest (left breast) always reads higher than expected (compare with the belt dosimeter). The reason here would appear to be a metal parachute harness holder located near this dosimeter- and consequent increase in the number of capture gamma rays.

One should also note that, for the standing phantom, the internal dosimeters are, within errors, rotationally invariant - due to the approximately constant amount of material surrounding them. When the phantom is prone the mid-gut dosimeter, as expected, gives a lower value, while the mid-brain detector shows little change.

(b) Bubble Dosimeter Results

Table 9 (a) again lists free-field and phantom dosimeter results with associated statistical uncertainties. For the wrist dosimeters, in the face-on and back-on orientations, there was some observed shielding of dosimeters either by each other or by the phantom itself. In the table, the values listed as (1) are closest to the core (i.e. nearest the thumb in the face-on orientation).

The dosimeter results again seem to follow expected trends with regard to phantom self-shielding. One major problem which had to be overcome in these experiments was the bubble dosimeter temperature dependance. In all experiments, the phantom was surrounded by a tent arrangement (see figs) in order to shade it from the sun and so prevent direct heating of the plastic, and thus the dosimeters. Temperatures were recorded at both external and internal phantom locations and the appropriate corrections made for each run. Desite these precautions, some heating may have occurred, however it is not considered a significant factor in this work. It should be noted that the sun shone directly on the side of the phantom facing the core for all runs.

Table 9 (b) lists the ratio of phantom dosimeter to free-field dosimeter response. Considering the unknown neutron energy spectrum at the phantom surface, and possible temperature effects we estimate the error at $\pm$ 10%.

In general, the albedo face of the phantom seems to give a slightly enhanced response compared to free-field. This may be due in part to downscattering of high-energy neutrons into the 200-500 keV range, where the bubble dosimeter response (per mrad) is somewhat higher.

The only two dosimeter sets which would appear to give somewhat inconsistent results are those located on the back for orientation (a) and on the right wrist for orientation (b). Both sets would appear to read somewhat low when compared to other corresponding locations.

(C) CR39 Results

Table (10) lists the results from the CR39 analysis, giving tracks cm^{-2} kWh^{-1} for each foil location, along with the three free-field components. These results are still somewhat preliminary and may undergo slight change after more extensive analysis (19), but this change is not expected to significantly affect these values. A table listing the ratios of phantom dosimeter to free-field dosimeter results is not presented here, because the non-isotropic detector response makes such absolute comparisons of dubious value.

An examination of the table reveals that the 'rotational reproducibility' of the results seems quite good, and the effects of phantom self-shielding are readily apparent. As opposed to the bubble case, the on-phantom dosimeter readings are slightly lower than their free-field counterparts (i.e. that component of the free-field dose matching their orientation). This may be due to the lower response of CR39 (relative to the bubbles) in the 200 keV - 300 keV region, and/or the non-isotropy factor.

As a somewhat qualitative analysis, we may look at either the belt or chest CR39 dosimeter and identify each with the x component of the dose in orientation (a). Making the assumption that the field at the phantom is more isotropic than its free field counterpart, due to scattering, then

$$\frac{D_x}{D_{total}} \qquad \frac{D_x}{D_{total}}$$

Or rewriting

$$\frac{(D_x)_{phantom}}{(Dx)_{FF}} \qquad \frac{(D_{total})_{phantom}}{(D_{total})_{FF}}$$

Identifying the LHS of the above with the CR39 results, and the RHS with the bubble results, we see that this relation is indeed true - the LHS averaging 0.76, compared to 1.04 for the R.H.S. Other orientations are somewhat more difficult to analyze. Clearly a full analysis relies on the energy and directional fluences to be calculated by SAI.

Conclusions

The current DREO dosimetry system-consisting of bubble, CR39 and TLD dosimeters - has proven capable of producing meaningful results at 400 m from a fission source. The effects of phantom orientation on dosimeter response were clearly demonstrated. Whether or not this experiment will constitute a benchmark experiment, or will need future refinement, will depend to a large degree on the accord between these results and theoretical calculations.

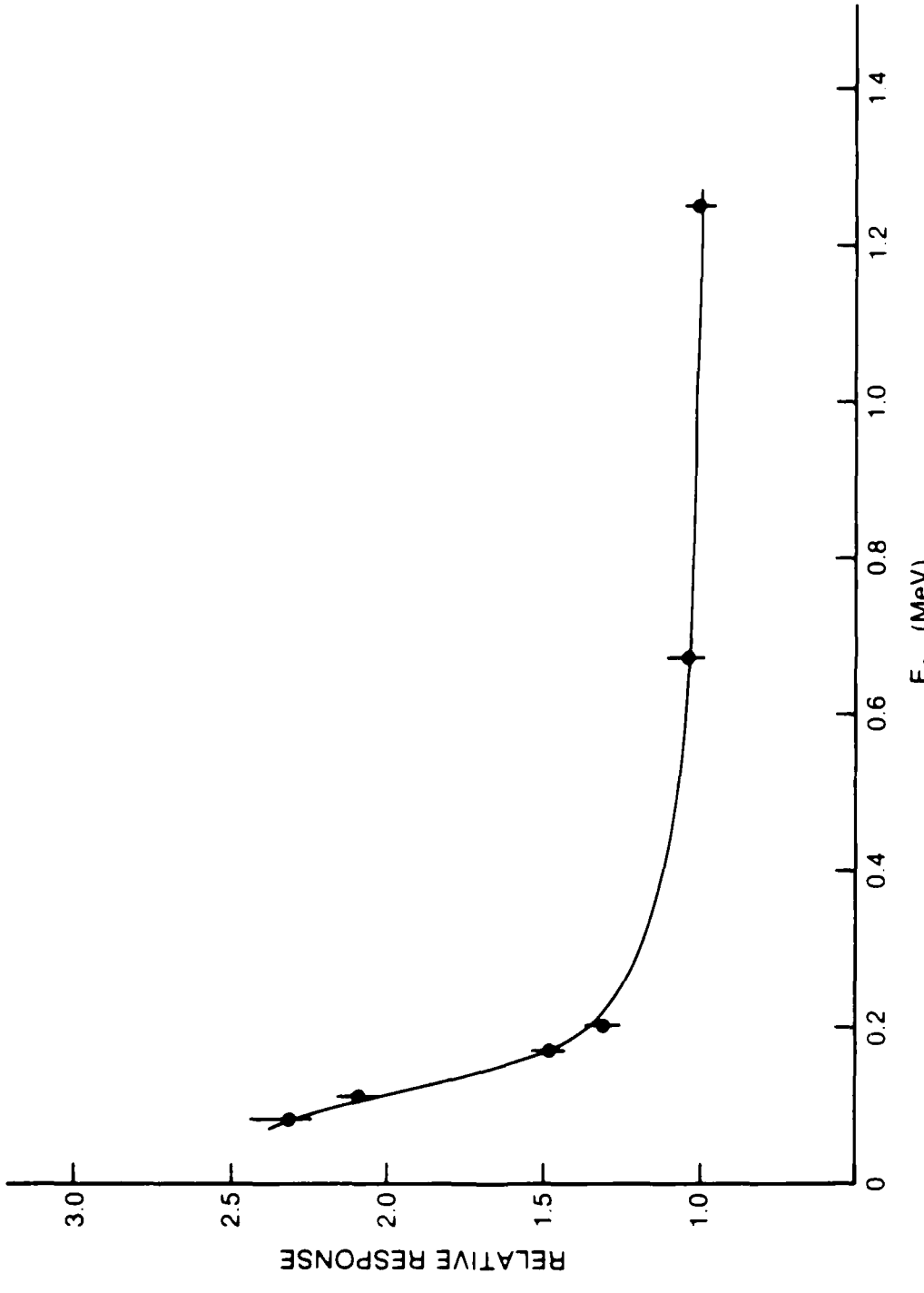

Figure 1 Kerma/Energy Response of CaF_2:Tm TLD's employed in this work

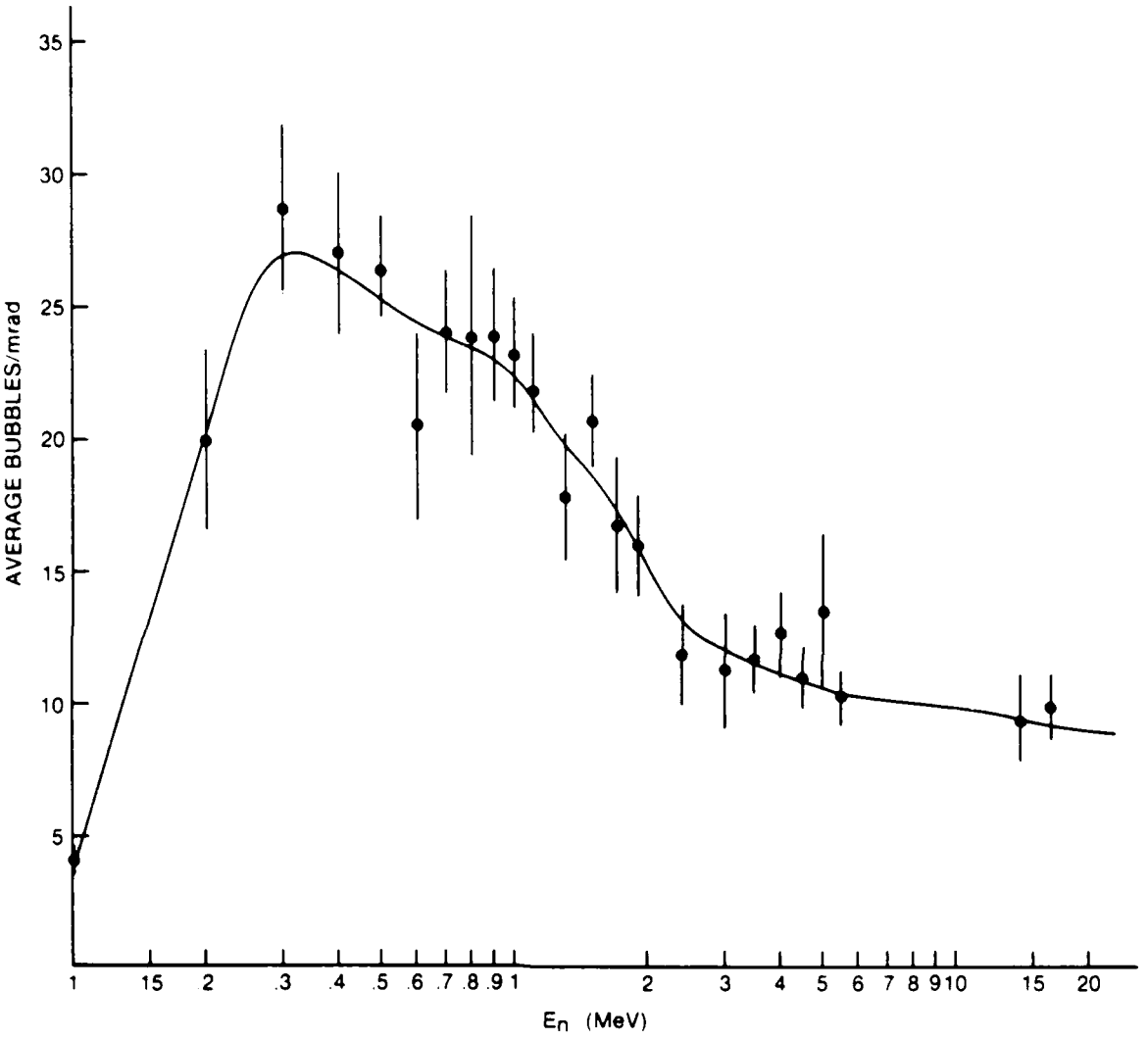

Figure 2 Kerma/Energy Response of Bubble Dosimeters employed in this work

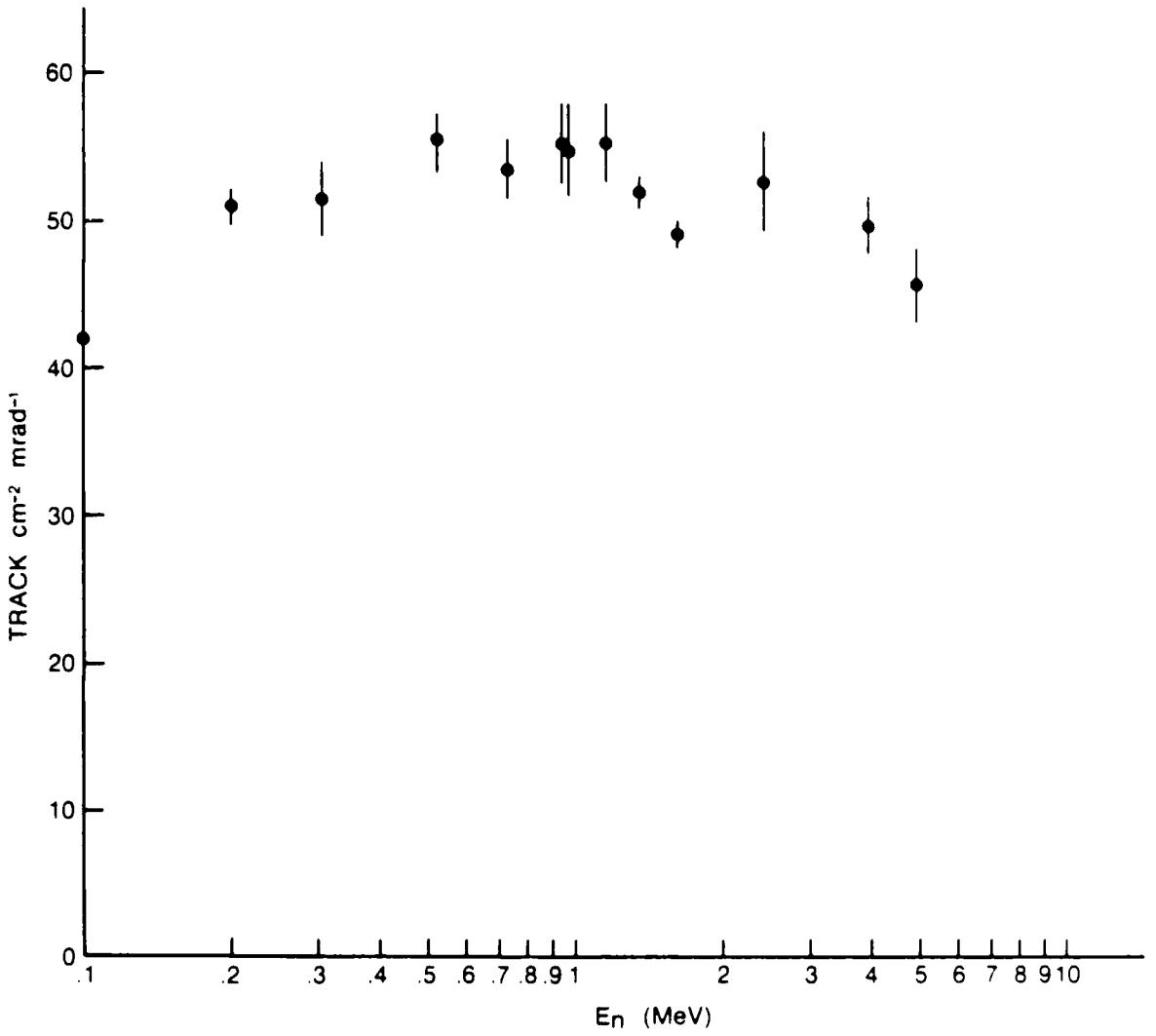

Figure 3 Kerma/Energy Response of CP39 Dosimeters employed in this work

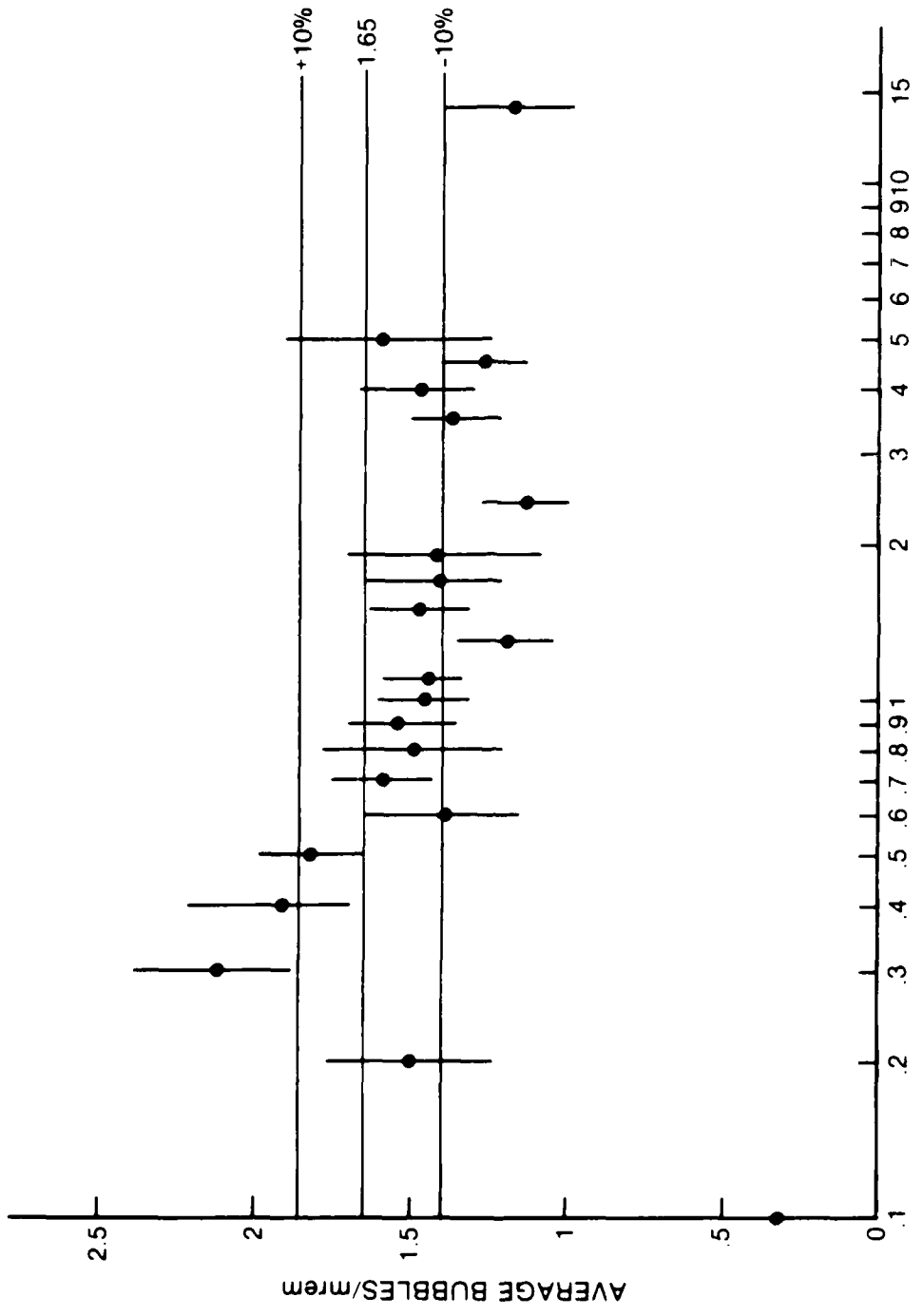

Figure 4 Dose Equivalent/Energy Response of Bubble Dosimeters Employed in this work

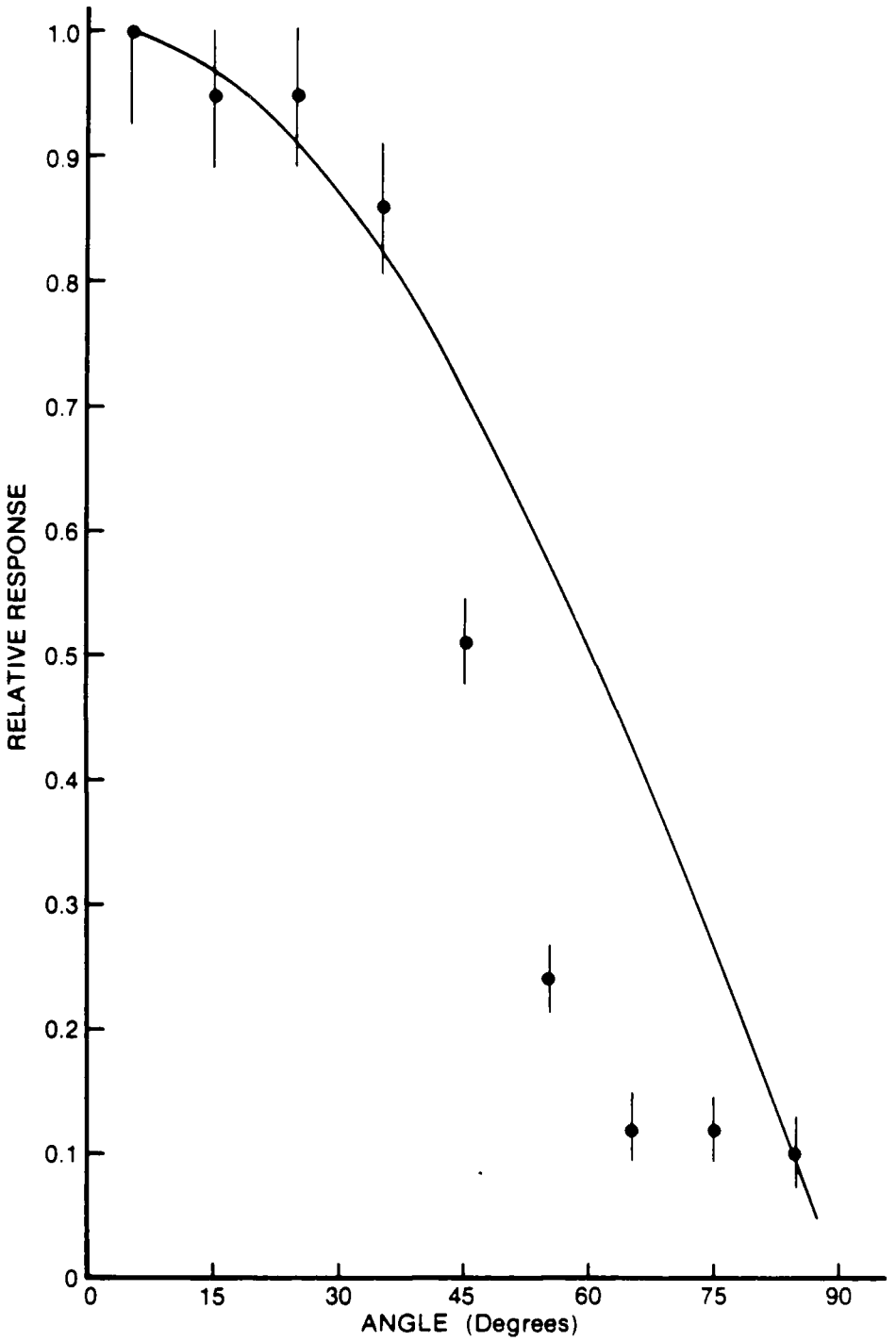

Figure 5 Angular Response of CR39 Dosimeters

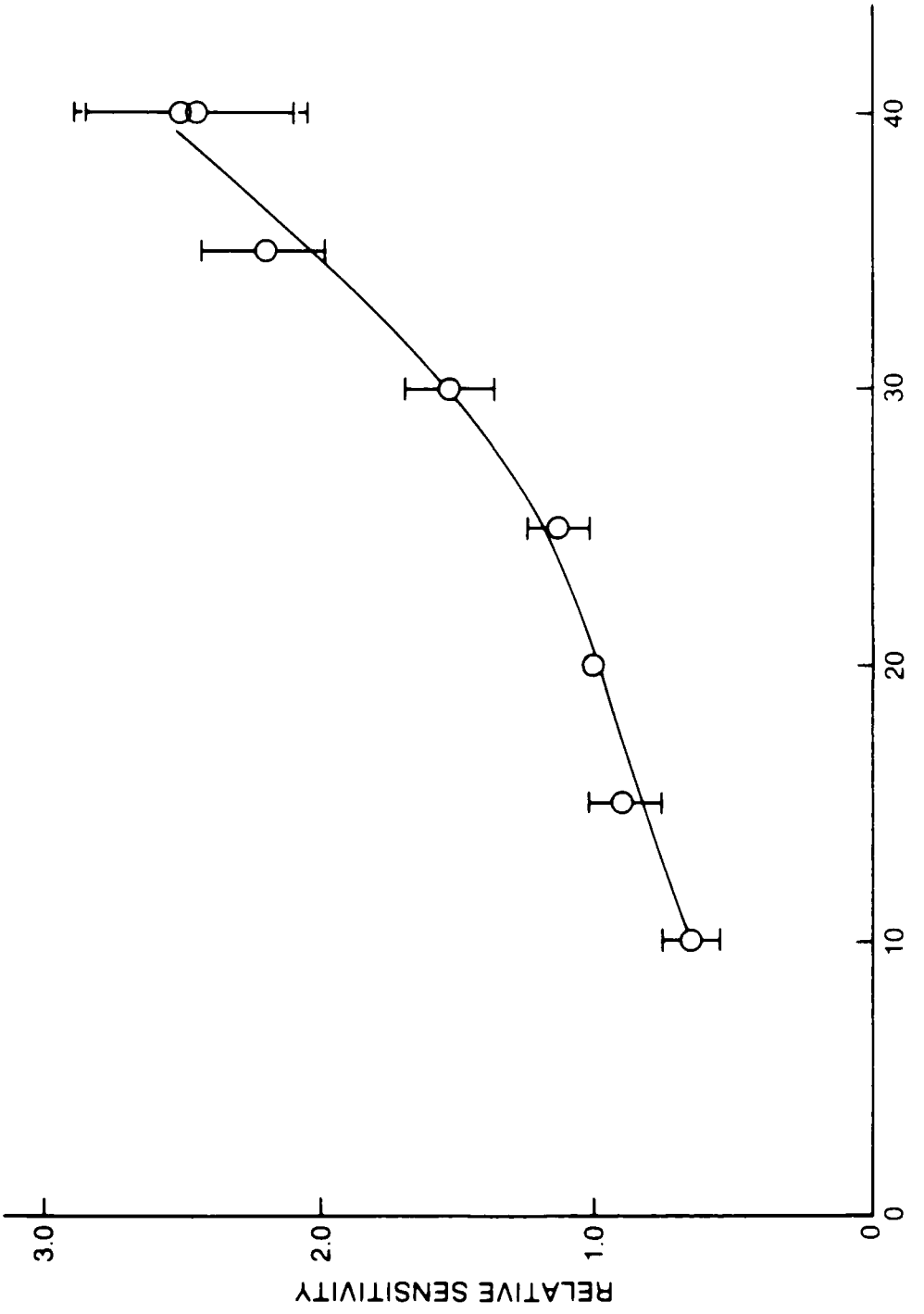

Figure 6 Temperature Dependence of Bubble Dosimeters

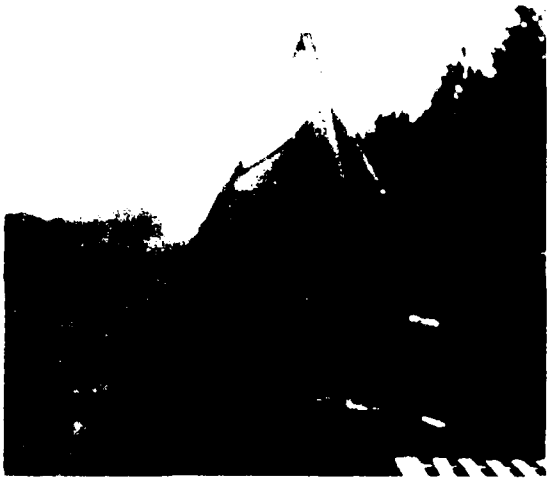

(a) Phantom facing core at 400 m. Note the sun-shielding plastic

(b) Side view of Phantom at 400 m. The French phantom used in the concurrent [illegible] is visible.

(c) Head of phantom disassembled to show position of mid-brain TLD

(d) Front view of Phantom. [illegible] chest [illegible] visible.

Figure 3

(a) Right wrist bubble dosimeters with CR39 and TLDs shown on phantom at 400 m.

(b) Left Wrist dosimeters

Figure 8

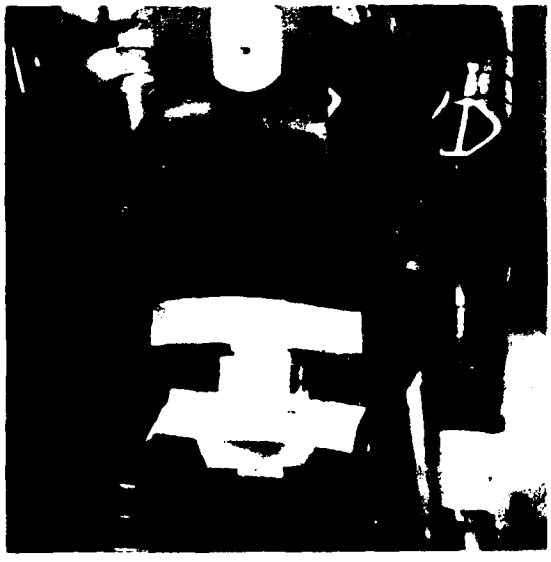

(a) Left Dosimeters on Phantom

(b) Lower Back Dosimeters on Phantom

Figure 9

References

1. NATO STANAG 2083 on "Commanders' guide on nuclear exposure of groups".

2. D.C. Kaul, Proceedings of the 1985 Workshop of the Research Study Group on the Assessment of Ionizing Radiation Injury in Nuclear Warfare NATO RSG-5, Panel VIII, Ottawa, September, 1985, pp. 88-102.

3. D.C. Kaul and R. Jarka, Science Applications Inc., Report No. SAI-121-748-1, October, 1977.

4. W.H. Scott, V.E. Staggs, D.C. Kaul, R. Jarka and S.Y. Chen, Science Applications Inc., Report No. SAI-133-80-269-LJ, February, 1980.

5. W.H. Scott and D.C. Kaul, Science Applications Inc., Report No. SAI-133-81-212-LJ, June, 1981.

6. A.H. Kazi, C.R. Heimbach, R.C. Harrison and H.A. Robitaille, Nuc. Sci. and Eng., 85, 1983, pp 371-386.

7. T. Cousins and L.P. Rushton, DREO Report No. 903, May, 1985.

8. H. Ing, K. Cundari, T. Cousins and L.P. Rushton, Atomic Energy of Canada Limited, Report No. AECL-9336, September, 1985.

9. A.H. Kazi, Aberdeen Proving Ground Memo for Record, STECS-AP (14-84), August, 1984.

10. International Commission on Radiological Protection, ICRP Publication 23, "Report of the Task Group on Reference Man", Permagon Press, Oxford, 1975.

11. Private Communication, P.A. Beeley, Royal Military College, Kingston, Ontario, March 1986.

12. R.A. Facey and R.A. Gravelle, DREO Report No. 682, August, 1973.

13. H. Ing and H.C. Birnboim, Nuc. Tracks, 8, 1984, pp 285-88.

14. L.P. Rushton, Proceedings of the 1985 Workshop of the Research Study Group on the Assessment of Ionizing Radiation Injury in Nuclear Warfare, NATO RSG-5, Panel VIII, September, 1985, pp 129-135.

15. D.C. Kaul (Science Applications Inc) personal communication to H.A. Robitaille.

16. H. Ing and W.G. Cross, Health Phys. 25, 1973, pp 291-297.

17. H. Ing and W.G. Cross, Int. Jour. Radiat. Isotopes, 24, 1973, pp 437-450.

18. H. Ing and S. Marka, "Compendium of Neutron Spectra in Criticality Accident Dosimetry", IAEA Tech. Report 180, IAEA, Vienna, 1978.

19. L.P. Rushton, DREO Report, to be published.

DOCUMENT CONTROL DATA

(Security classification of title, body of abstract and indexing annotation must be entered when the overall document is classified)

1. ORIGINATOR (the name and address of the organization preparing the document. Organizations for whom the document was prepared, e.g. Establishment sponsoring a contractor's report, or tasking agency, are entered in section 8.)

Department of National Defence
Defence Research Establishment Ottawa
Ottawa, Ontario
K1A 0Z4

2. SECURITY CLASSIFICATION (overall security classification of the document including special warning terms if applicable)

UNCLASSIFIED

3 TITLE (the complete document title as indicated on the title page. Its classification should be indicated by the appropriate abbreviation (S,C,R or U) in parentheses after the title.)

Anthropomorphic Phantom Radiation Dosimetry at the NATO Standard Reference Point at Aberdeen Proving Ground

4. AUTHORS (Last name, first name, middle initial. If military, show rank, e.g. Doe, Maj. John E.)

Cousins, T., and Rushton, L.P.

5. DATE OF PUBLICATION (month and year of publication of document)	6a. NO. OF PAGES (total containing information. Include Annexes, Appendices, etc.)	6b. NO. OF REFS (total cited in document)
March 1987	26	19

7. DESCRIPTIVE NOTES (the category of the document, e.g. technical report, technical note or memorandum. If appropriate, enter the type of report, e.g. interim, progress, summary, annual or final. Give the inclusive dates when a specific reporting period is covered.)

DREO Report

8. SPONSORING ACTIVITY (the name of the department project office or laboratory sponsoring the research and development. Include the address.)

9a. PROJECT OR GRANT NO. (if appropriate, the applicable research and development project or grant number under which the document was written. Please specify whether project or grant)	9b. CONTRACT NO. (if appropriate, the applicable number under which the document was written)
051LA12	

10a. ORIGINATOR'S DOCUMENT NUMBER (the official document number by which the document is identified by the originating activity. This number must be unique to this document.)	10b. OTHER DOCUMENT NOS. (Any other numbers which may be assigned this document either by the originator or by the sponsor)
DREO Report 968	

11. DOCUMENT AVAILABILITY (any limitations on further dissemination of the document, other than those imposed by security classification)

(X) Unlimited distribution
( ) Distribution limited to defence departments and defence contractors; further distribution only as approved
( ) Distribution limited to defence departments and Canadian defence contractors; further distribution only as approved
( ) Distribution limited to government departments and agencies; further distribution only as approved
( ) Distribution limited to defence departments; further distribution only as approved
( ) Other (please specify):

12. DOCUMENT ANNOUNCEMENT (any limitation to the bibliographic announcement of this document. This will normally correspond to the Document Availability (11). However, where further distribution (beyond the audience specified in 11) is possible, a wider announcement audience may be selected.)

UNCLASSIFIED

SECURITY CLASSIFICATION OF FORM

13. ABSTRACT (a brief and factual summary of the document. it may also appear elsewhere in the body of the document itself. it is highly desirable that the abstract of classified documents be unclassified. Each paragraph of the abstract shall begin with an indication of the security classification of the information in the paragraph (unless the document itself is unclassified) represented as (S), (C), (R), or (U). It is not necessary to include here abstracts in both official languages unless the text is bilingual).

(U) As part of the NATO Dosimetry Intercomparison Project, a series of experiments were conducted at Aberdeen Proving Ground in September 1986 in order to determine neutron and gamma-ray doses delivered to various internal and external locations on an anthropomorphic phantom from a fission source. Thus the efect of such parameters as self-shielding by the body on dosimeter reading may be determined. The results will be used eventually to validate computer simulations of the Aberdeen environment in order to understand completely the correlation between dosimeter reading and bone marrow dose, or other parameters relating to performance decrement.

14. KEYWORDS, DESCRIPTORS or IDENTIFIERS (technically meaningful terms or short phrases that characterize a document and could be helpful in cataloguing the document. They should be selected so that no security classification is required. Identifiers, such as equipment model designation, trade name, military project code name, geographic location may also be included. If possible, keywords should be selected from a published thesaurus, e.g. Thesaurus of Engineering and Scientific Terms (TEST) and that thesaurus identified. If it is not possible to select indexing terms which are Unclassified, the classification of each should be indicated as with the title.)

Neutron
Gamma-ray
Anthrompomorphic Phantom
TLD
CR39
Bubble Dosimeter
Fission

UNCLASSIFIED

SECURITY CLASSIFICATION OF FORM

END

DATE

FILMED

DTIC

4/88